

# THE JET/ENVIRONMENT DENSITY RATIO OF STELLAR JETS

A.C. Raga

Department of Mathematics, UMIST, U.K.

and

A. Noriega-Crespo

Astronomy Department, University of Washington, U.S.A.

Received 1993 April 14

## RESUMEN

El cociente entre la densidad de chorros estelares y la densidad del material circundante es uno de los parámetros más importantes, y posiblemente es también el más incierto de los parámetros físicos de los chorros estelares. Presentamos un método sencillo para determinar este cociente de densidades, que puede ser usado para objetos en que el choque a proa ("bowshock") y el disco de Mach en la cabeza del jet están resueltos en imágenes de banda angosta en  $H\alpha$  y  $[S II]\lambda\lambda 6717+31$ . Nuestro método también sirve para determinar los valores de las velocidades de choque del disco de Mach y del choque a proa.

Mediante la aplicación de este método a las observaciones de HH 111V de Reipurth, Raga, & Heathcote (1992) se obtiene un cociente de densidades (entre el chorro y el material circundante) igual a 23. Los valores de las velocidades de choque son  $v_{js} \approx 25 \text{ km s}^{-1}$  y  $v_{bs} = 110 \text{ km s}^{-1}$  para el disco de Mach y para el choque a proa (respectivamente). Estos valores son consistentes con el balance de presión hidrodinámica que debe ocurrir entre ambos lados de una superficie de trabajo. Este resultado parece confirmar la identificación del choque a proa y del disco de Mach de HH 111V.

## ABSTRACT

The jet-to-environment density ratio is one of the most important, and possibly the most uncertain of the parameters of jets from young stars. We present a simple method for determining this density ratio, which can be used for objects in which the bowshock and the terminal Mach disk (or "jet shock") in the head of the jet are observationally resolved in  $H\alpha$  and  $[S II]\lambda\lambda 6717+31$  narrowband images. Our method also yields values for the shock velocities of the bowshock and the jet shock.

An application of this method to the HH 111 observations of Reipurth, Raga, & Heathcote (1992) gives a jet-to-environment density ratio of 23 at the position of HH 111V. The values obtained for the shock velocities are  $v_{js} \approx 25 \text{ km s}^{-1}$  and  $v_{bs} \approx 110 \text{ km s}^{-1}$  for the jet shock and for the bowshock (respectively). The obtained density ratio and shock velocities are consistent with ram pressure balance across the working surface, which gives credibility to the identification of the jet shock and bowshock emission in the HH 111V observations.

**Key words:** ISM-JETS AND OUTFLOWS — ISM-KINEMATICS AND DYNAMICS — SHOCK WAVES

## 1. INTRODUCTION

The velocity of propagation of the head of a jet is determined by the velocity of the jet flow and by the jet-to-environment density ratio  $\rho_j/\rho_e$  at the position of the head of the jet ( $\rho_j/\rho_e$  is a function of distance from the source, as both the density of the

jet and of the environment in principle depend on distance from the source). These parameters can be used to determine the motion of the head of the jet using the condition of ram-pressure balance across the two-shock working surface (see, e.g., the review of Dyson 1987, and references therein).

It has recently been argued that jets from young stars appear to be propagating into an environment that is also moving away from the central source (see, e.g., Raga et al. 1987, Morse et al. 1992). This result is consistent with the interpretation of the characteristics of Herbig-Haro (HH) objects as the result of episodic ejections from young stellar objects (see, e.g., Reipurth 1989a, Raga et al. 1990, Hartigan & Raymond 1993), in which subsequent “outflow events” produce two-shock working surfaces (which have a leading “bowshock” and a trailing “jet shock”) that travel into the slow “tail” of the previous outflow episode.

From comparisons between theoretical models and spectroscopic observations, it has been argued that the emission from the working surface is dominated by the contribution from the bowshock (Solf, Böhm, & Raga 1986; Hartigan, Raymond, & Hartmann 1987). This result can be interpreted as directly implying that the density of the flow upstream of the working surface (i.e., towards the source) is considerably higher than the density of the material into which the working surface is travelling (Hartigan 1989; Raga & Kofman 1992).

Even though it is now quite generally accepted that many HH objects correspond to working surfaces with upstream-to-downstream density ratios greater than one, a precise determination of this ratio is quite difficult. This is due to the fact that in most cases apparently only the bowshock is observed, and a direct observation of the jet shock is also necessary for a determination of the density ratio.

However, recent observations show that in a few HH objects the emission from the jet shock and the bowshock can be separated (e.g., HH 47A: Reipurth & Heathcote 1991; HH 34S: Reipurth & Heathcote 1992). The most striking example is probably HH 111V (the leading “head” of the blue-shifted lobe of the HH 111 system, Reipurth 1989b), in which a very clear jet shock-bowshock separation is apparently observed in the subtraction of an H $\alpha$  from a [S II] $\lambda\lambda 6717+31$  image (Reipurth, Raga, & Heathcote 1992).

In this paper we develop a simple prescription (based on the plane-parallel shock models of Hartigan et al. 1987) for calculating the shock velocities of the bowshock and the jet shock, together with the up-to-downstream density ratio from the observed H $\alpha$  and [S II] $\lambda\lambda 6717+31$  intensities of the bowshock and the jet shock. We then apply this prescription to the HH 111V observations of Reipurth et al. (1992).

## 2. H $\alpha$ AND [S II] EMISSION FROM PLANE-PARALLEL SHOCKS

Let us assume that we have an observation of the on-axis H $\alpha$  and [S II] $\lambda\lambda(6717+31)$  intensities

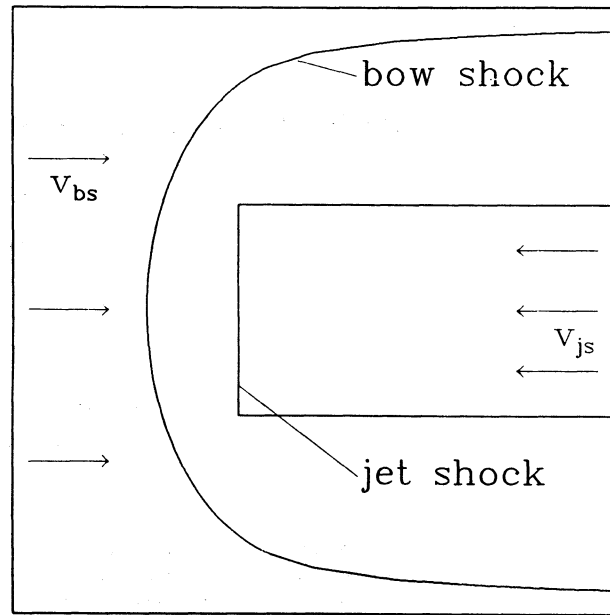


Fig. 1. Schematic diagram of the “jet shock + bowshock” structure formed at the head of a jet. The direction away from the outflow source is towards the left. In a frame of reference at rest with respect to the working surface, the jet beam has a velocity  $v_{js} = v_j - v_{ws}$  (directed away from the source), where  $v_j$  and  $v_{ws}$  are the velocities of the jet beam material and the working surface (respectively) relative to the outflow source. In the same reference frame (moving with the working surface), the material to the left of the bowshock has a velocity  $v_{bs} = v_{ws} - v_p$ , where  $v_p$  is the velocity relative to the outflow source of the material into which the jet head is moving.

of the bowshock and the jet shock of a working surface (see Figure 1). In the limit of short cooling distances, the emission behind these two shocks can be approximately modelled with plane-parallel shock calculations, such as the ones of Hartigan et al. (1987). Carrying out power law fits to the numerical results of this paper, we find that the H $\alpha$  and the [S II] $\lambda\lambda(6717+31)$  emission per unit time and area of a radiative shock is approximately given by:

$$I_{H\alpha} = C_{H\alpha} \left( \frac{n_{pre}}{100 \text{ cm}^{-3}} \right) \left( \frac{v_{shock}}{1 \text{ km s}^{-1}} \right)^{\alpha_{H\alpha}}, \quad (1)$$

$$I_{[S II]} = C_{[S II]} \left( \frac{n_{pre}}{100 \text{ cm}^{-3}} \right) \left( \frac{v_{shock}}{1 \text{ km s}^{-1}} \right)^{\alpha_{[S II]}}, \quad (2)$$

where  $n_{pre}$  is the pre-shock (ion+atom) number density, and  $v_{shock}$  is the shock velocity. The values of the constants  $C$  and  $\alpha$  are given in Table 1 for three different ( $v_{min}$ ,  $v_{max}$ ) shock velocity

TABLE 1

COEFFICIENTS FOR LINE INTENSITY FITS

$v_{min}$ (km s <sup>-1</sup> )	$v_{max}$ (km s <sup>-1</sup> )	$C_{H\alpha}$ (erg cm <sup>-2</sup> s <sup>-1</sup> )	$C_{[S II]}$ (erg cm <sup>-2</sup> s <sup>-1</sup> )	$\alpha_{H\alpha}$	$\alpha_{[S II]}$
20.0	81.3	$1.86 \times 10^{-10}$	$6.32 \times 10^{-7}$	3.49	1.02
81.3	117.5	$8.71 \times 10^{-4}$	$3.66 \times 10^{-17}$	0.00	6.38
117.5	200.0	$5.13 \times 10^{-8}$	$3.03 \times 10^{-8}$	2.04	2.07

ranges. The line intensities predicted by Hartigan et al. (1987) are shown together with the power law fits (equations 1 and 2, and Table 1) in Figure 2. From this figure, we see that the maximum deviation between the model results and the power law fits is of  $\approx 15\%$ .

We should note that equation (2) is appropriate only as long as the [S II] line emission does not deviate considerably from the low density regime. We find that this condition is satisfied for pre-shock densities  $n_{pre} < 100 \text{ cm}^{-3}$  for shock velocities  $v_{shock} < 200 \text{ km s}^{-1}$ . However, for slower shocks with  $v_{shock} < 50 \text{ km s}^{-1}$ , equation (2) is approximately valid for pre-shock densities  $n_{pre} < 1000 \text{ cm}^{-3}$ . These limits for the validity of equation (2) should be kept in mind when using this interpolation for the [S II] emission.

### 3. DETERMINATION OF THE WORKING SURFACE PARAMETERS

Let us now assume that we have observed the spatially resolved H $\alpha$  and [S II] emission of both the bowshock and the jet shock. We can then use the observations to compute the line ratios:

$$r_b = I_{[S II]}^{(b)} / I_{H\alpha}^{(b)}, \quad (3a)$$

$$r_j = I_{[S II]}^{(j)} / I_{H\alpha}^{(j)}, \quad (3b)$$

$$r_{jb} = I_{[S II]}^{(j)} / I_{[S II]}^{(b)}, \quad (3c)$$

where the subscripts  $b$  and  $j$  denote the intensities observed for the bowshock and the jet shock, respectively. It is also possible to define a jet-to-bowshock H $\alpha$  ratio (in the same way as the equivalent [S II] ratio defined in 3c), but this fourth line ratio does not provide any independent information from that already contained in the ratios given by equation (3).

It is clear that the [S II]/H $\alpha$  ratios (3a and 3b) can be used together with the fits given by equations (1) and (2) to obtain the shock velocities  $v_{js}$  and

$v_{bs}$  for both the bowshock and the jet shock (see Figure 1). This is quite straightforward, because the preshock density cancels out when the line ratios are calculated, and an equation is left that can be straightforwardly inverted to obtain the value of the shock velocity.

However, a small complication arises due to the fact that the coefficients of the interpolation formulae (1 and 2) are different for different velocity regimes (see § 2 and Table 1). This results in the fact that for most values of the [S II]/H $\alpha$  line ratio one obtains two possible solutions (a “fast” and a “slow” solution) for the shock velocity. The existence of these two solutions can be clearly seen from Figure 2.

Once we have determined the possible (“fast” and “slow”) solutions for the shock velocities,  $v_{bs}$  and  $v_{js}$ , we can use the jet-to-bowshock [S II] line ratio (equation 3c) to determine the ratio between the pre-jet shock and pre-bowshock densities. In this way we can compute the ratio  $\rho_j/\rho_e$  of the density of the jet (just upstream of the working surface) to the

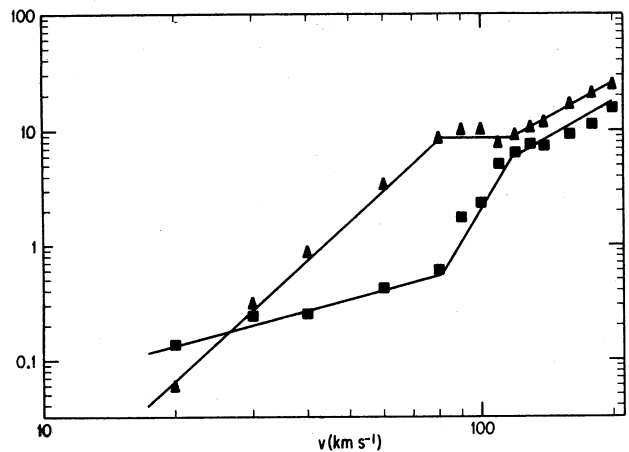


Fig. 2. H $\alpha$  (skeleton triangles) and [S II] $\lambda\lambda 6717+31$  (solid squares) emission as a function of shock velocity from the  $n_{pre} = 100 \text{ cm}^{-3}$  models of Hartigan, Raymond, & Hartmann (1987). The continuous lines are the power law fits discussed in the text. The line intensities are given in  $10^{-4} \text{ erg cm}^{-2} \text{ s}^{-1}$ .

density of the surrounding environment (which, as we have discussed in § 1, could actually correspond to the “tail” of a previous outflow episode).

In the following section, we apply this method for determining the shock velocities,  $v_{bs}$  and  $v_{js}$ , and the density ratio,  $\rho_j/\rho_e$ , to the case of HH 111V.

#### 4. THE PARAMETERS OF HH 111V

HH 111V is a blueshifted, bow-shaped structure located approximately  $140''$  West of the source of the HH 111 outflow (Reipurth 1989b). The high resolution H $\alpha$  and [S II] NTT images of Reipurth et al. (1992) show a low excitation structure upstream of the bowshock, which these authors have identified as the terminal Mach disk (or “jet shock”) of the HH 111V working surface. These images are calibrated (relative to each other), so that they can be used to obtain the line ratios required for applying the method described in § 3. From the data of Reipurth et al. (1992, Figure 9), we then obtain the line ratios  $r_b = 0.46$ ,  $r_j = 1.16$  and  $r_{jb} = 0.98$  (these ratios are defined by equation 3).

The possible shock velocities for the HH 111V working surface are limited by another observational result. Noriega, Garnavich, & Raga (1993) have obtained high signal-to-noise blue spectra of this object, and have found at most only marginally detectable [O III] $\lambda 5007$  emission. This limits the possible shock velocities to  $< 100 \text{ km s}^{-1}$ , as higher velocity shocks produce very strong [O III] $\lambda 5007$  emission (Hartigan et al. 1987), which is clearly not observed in HH 111V.

From the  $r_b = 0.46$  value, we determine (using equations 1 and 2) the two possible solutions for the shock velocity  $v_{bs}$  of the bowshock:  $v_{bs}^{(1)} = 37 \text{ km s}^{-1}$ , and  $v_{bs}^{(2)} = 110 \text{ km s}^{-1}$ . The higher shock velocity lies just above the limit imposed by the observed lack of [O III] $\lambda 5007$  emission (see above), but it cannot be eliminated due to the uncertainty of our line ratio determinations. Even more, this higher shock velocity is in surprising agreement with the results of Morse (1992), who has found that the spatially resolved line profiles of HH 111V can be fitted with a model of a  $100 \text{ km s}^{-1}$  bowshock. This result can be used to discriminate between the two possible velocities deduced from the [S II]/H $\alpha$  line ratio to conclude that the bowshock approximately has a velocity  $v_{bs} = 110 \text{ km s}^{-1}$ .

From the  $r_j = 1.16$  value, we determine (using equations 1 and 2) that there is only one possible solution (within the velocity range of our power law fits) for the shock velocity of the jet shock:  $v_{js} = 25 \text{ km s}^{-1}$ . The plane-parallel shock models of Hartigan et al. (1987) show that a [S II]/H $\alpha$  ratio of  $\approx 1.1$  is also obtained for a shock velocity  $\approx 260 \text{ km s}^{-1}$  (outside of the range of validity of our

fits, see Table 1). This shock velocity, however, is clearly eliminated by the lack of [O III] emission in HH 111V (see above).

With the  $r_{jb} = 0.98$  jet shock-to-bowshock [S II] line ratio, the bowshock velocity  $v_{bs} = 110 \text{ km s}^{-1}$  and the jet shock velocity  $v_{js} = 25 \text{ km s}^{-1}$ , from equations (1) and (2) we can determine the value of the jet-to-environment density ratio:  $(\rho_j/\rho_e)^{(2)} = 23$ .

We find that these determinations of  $v_{js}$ ,  $v_{bs}$  and  $\rho_j/\rho_e$  are surprisingly consistent with a working surface model for HH 111V in the following sense. As discussed in § 1, there is an approximate ram pressure balance between the flow upstream and downstream of the working surface:

$$\rho_j v_{js}^2 = \rho_e v_{bs}^2. \quad (4)$$

Using the  $v_{bs} = 110 \text{ km s}^{-1}$  and  $v_{js} = 25 \text{ km s}^{-1}$  shock velocities (deduced from the [S II]/H $\alpha$  line ratios), from equation (4) we then obtain a density ratio  $\rho_j/\rho_e = 19$ , which is in excellent agreement with the value determined from the jet-to-bowshock [S II] line ratio ( $\rho_j/\rho_e = 23$ , see above).

#### 5. CONCLUSIONS

We have presented a method to obtain the shock velocities and density ratio across a working surface from spatially resolved observations of the H $\alpha$  and [S II] $\lambda\lambda 6717+31$  intensities of the bowshock and the jet shock. This method can be applied to the observations of HH 111V of Reipurth et al. (1992), which do show spatially resolved structures which can be interpreted as being the bowshock and the jet shock of a working surface.

For HH 111V we then obtain shock velocities of  $v_{bs} = 110 \text{ km s}^{-1}$  and  $v_{js} = 25 \text{ km s}^{-1}$  for the jet shock and the bowshock (respectively) and a density ratio  $\rho_j/\rho_e = 23$  across the working surface (with the lower density region in the direction away from the source). We find that these values are surprisingly consistent with the condition of ram pressure balance across the working surface.

If we take the estimate of  $\approx 10 \text{ cm}^{-3}$  for the number density of the environment around HH 111V from Raga & Binette (1991), we conclude that the jet has a number density of  $\approx 230 \text{ cm}^{-3}$ . This value is very similar to the electron density determined by Reipurth (1989b) for the condensation HH 111T, which is the knot of the HH 111 jet directly upstream (approximately  $8''$ ) of HH 111V.

It is interesting to note that proper motion and radial velocity measurements imply that HH 111V is moving at a velocity of  $v_{ws} \approx 400 \text{ km s}^{-1}$  away from the central source (Reipurth et al. 1992). Our shock velocity determinations then imply that

HH 111V is the result of the interaction of a beam of velocity  $v_j = v_{ws} + v_{js} = 425 \text{ km s}^{-1}$  with a previously ejected outflow of velocity  $v_p = v_{ws} - v_{bs} = 290 \text{ km s}^{-1}$  (see Figure 1). It will be interesting to see if future high signal-to-noise, high resolution spectroscopic observations of the region around HH 111V do show material at these velocities upstream and downstream of the working surface.

The authors would like to thank Prof. J. Dyson for helpful comments. ANC's work was funded by NSF grant AST-91-14888. Part of this work was carried out during a visit of ANC to the Mathematics Department at UMIST.

#### REFERENCES

- Dyson, J.E. 1987, in IAU Symposium 122, Circumstellar Matter, eds. I. Appenzeller & C. Jordan (Dordrecht: Reidel), p. 159
- Hartigan, P. 1989, *ApJ*, 339, 987
- Hartigan, P., Raymond, J.C., & Hartmann, L. 1987, *ApJ*, 316, 323
- Hartigan, P., & Raymond, J.C. 1993, *ApJ*, in press
- Morse, J.A. 1992, Ph. D. Thesis, The University of North Carolina, Chapel Hill
- Morse, J.A., Hartigan, P., Cecil, G., Raymond, J.C., & Heathcote, S. 1992, *ApJ*, 339, 231
- Noriega-Crespo, A., Garnavich, P.M., & Raga, A.C. 1993, *AJ*, in press
- Raga, A.C., Mateo, M. Böhm, K.H., & Solf, J. 1987, *AJ*, 95, 1783
- Raga, A.C., Cantó, J., Binette, L., & Calvet, N. 1990, *ApJ*, 364, 601
- Raga, A.C., & Binette, L. 1991, *RevMexAA*, 22, 265
- Raga, A.C., & Kofman, L. 1992, *ApJ*, 386, 222
- Reipurth, B. 1989a, in ESO Workshop on Low Mass Star Formation and Pre-Main Sequence Objects, ed. B. Reipurth (Garching: ESO), p. 247
- \_\_\_\_\_. 1989b, *Nat*, 340, 42
- Reipurth, B., Raga, A.C., & Heathcote, S. 1992, *ApJ*, 392, 145
- Reipurth, B., & Heathcote, S. 1991, *A&A*, 246, 511
- \_\_\_\_\_. 1992, *A&A*, 257, 693
- Solf, J., Böhm, K.H., & Raga, A.C. 1986, *AJ*, 305, 795
- Alberto Noriega-Crespo: Astronomy Department, FM-20, University of Washington, Seattle, WA 98195, USA.
- Alejandro C. Raga: Astrophysics Group, Department of Mathematics, UMIST, P.O. Box 88, Manchester M60 1QD, U.K.